NREL/TP-214-4468 • UC Category: 273 • DE92001168

Role of Polycrystallinity in CdTe and $CuInSe_2$ Photovoltaic Cells

Annual Subcontract Report 1 April, 1990 - 31 March 1991

NREL/TP--214-4468

DE92 001168

J. R. Sites
Colorado State University
Fort Collins, Colorado

NREL technical monitor: H.S. Ullal

National Renewable Energy Laboratory
(formerly the Solar Energy Research Institute)
1617 Cole Boulevard
Golden, Colorado 80401-3393
A Division of Midwest Research Institute
Operated for the U.S. Department of Energy
under Contract No. DE-AC02-83CH10093

Prepared under Subcontract No. XC-0-10046-1

November 1991

On September 16, 1991, the Solar Energy Research Institute was designated a national laboratory, and its name was changed to the National Renewable Energy Laboratory.

NOTICE

Printed in the United States of America
Available from:
National Technical Information Service
U.S. Department of Commerce
5285 Port Royal Road
Springfield, VA 22161

Price: Microfiche A01
Printed Copy A03

Codes are used for pricing all publications. The code is determined by the number of pages in the publication. Information pertaining to the pricing codes can be found in the current issue of the following publications which are generally available in most libraries: *Energy Research Abstracts (ERA)*; *Government Reports Announcements* and Index (*GRA* and I); *Scientific and Technical Abstract Reports (STAR)*; and publication NTIS-PR-360 available from NTIS at the above address.

SUMMARY

The polycrystalline nature of thin-film CdTe and $CuInSe_2$ solar cells continues to be a major factor in several individual losses that limit overall cell efficiency. This report describes progress in the quantitative separation of these losses including both measurement and analysis procedures. It also applies these techniques to several individual cells to help document the overall progress with CdTe and $CuInSe_2$ cells. Notably, CdTe cells from Photon Energy have reduced window photocurrent loss to 1 mA/cm^2, those from USF have achieved a maximum power voltage of 693 mV, and $CuInSe_2$ cells from ISET have shown a hole density as high as $7x10^{16}$ cm^{-3}, implying a significant reduction in compensation.

TABLE OF CONTENTS

FIGURES

TABLES

1. INTRODUCTION

Comparative quantitative analysis of individual loss mechanisms in thin-film polycrystalline solar cells continues to become more successful as cells improve in efficiency and as measurement and analysis techniques become more refined. The following sections of this report summarize our results from a variety of CdTe and $CuInSe_2$ solar cells.

Section 2 gives an outline of our approach to polycrystalline cell analysis. Section 3 looks in detail at several CdTe cells, and Section 4 at $CuInSe_2$. Section 5 reports on a set of $CuInSe_2$ annealing studies. Finally, Section 6 describes some of the upgrades made to our measurement facility during the past year.

The experimental and analytical studies described were performed in large part by two research students, Rick Sasala and Xiaoxiang Liu. Some of the experimental data used was provided by Keith Emery of SERI or taken from the open literature. Cells used in the measurement and analysis were fabricated at the Ametek Applied Materials Laboratory, Georgia Institute of Technology, the Institute for Energy Conversion, International Solar Electric Technology, Microchemistry Ltd., Photon Energy, and the University of South Florida. Colleagues at both SERI and the other laboratories above have contributed numerous suggestions and stimulating discussion to the analysis reported here.

2. COMPARATIVE LOSS ANALYSIS

For comparison purposes it is convenient to define a target cell. We have been using a hypothetical 15% efficiency (active area) targets for both $CuInSe_2$ and CdTe using the parameters in Table 2-1. The parameters were chosen somewhat arbitrarily, based on values that the better cells in each case seemed to be approaching and what might be expected for the respective bandgaps. When cell efficiencies surpass 15%, we expect to define new target parameters, probably using 18% as the next milestone.

Table 2-1. Parameters Used for Target Cells

	$CuInSe_2$	CdTe
J_L [mA/cm^2]	42	25
V_{OC} [mV]	500	800
A-factor	1.7	2.2
R_S	0	0
r_S	∞	∞
Fill factor	0.715	0.75
Efficiency [%]	15	15

Our target photocurrents compare with maximum values of 47 and 30½ mA/cm^2 respectively based on a standard global 100 mW/cm^2 solar spectrum [1] and the respective bandgaps of $CuInSe_2$ and CdTe. The target values assume losses from reflection, window absorption, and recombination relating to deeply penetrating long-wavelength photons that are distributed roughly as shown in Table 2-2. The target reflection loss for CdTe is slightly higher since at present a superstrate glass configuration without AR coating typically produces 5-6% reflection. In the field, of course, substrate $CuInSe_2$ cells would likely have an encapsulant with a similar reflection.

Table 2-2. Differences Between Target and Maximum Photocurrents

	$CuInSe_2$	CdTe
Target Photocurrent [mA/cm^2]	42	25
Reflection Loss	1½	2
Window Absorption Loss	1½	1½
Deep Penetration Loss	2	2
Maximum Photocurrent	47	30½

The forward current ($J + J_L$) vs. voltage curves corresponding to the target cell parameters of Table 2-1 are shown in Fig. 2-1. This type

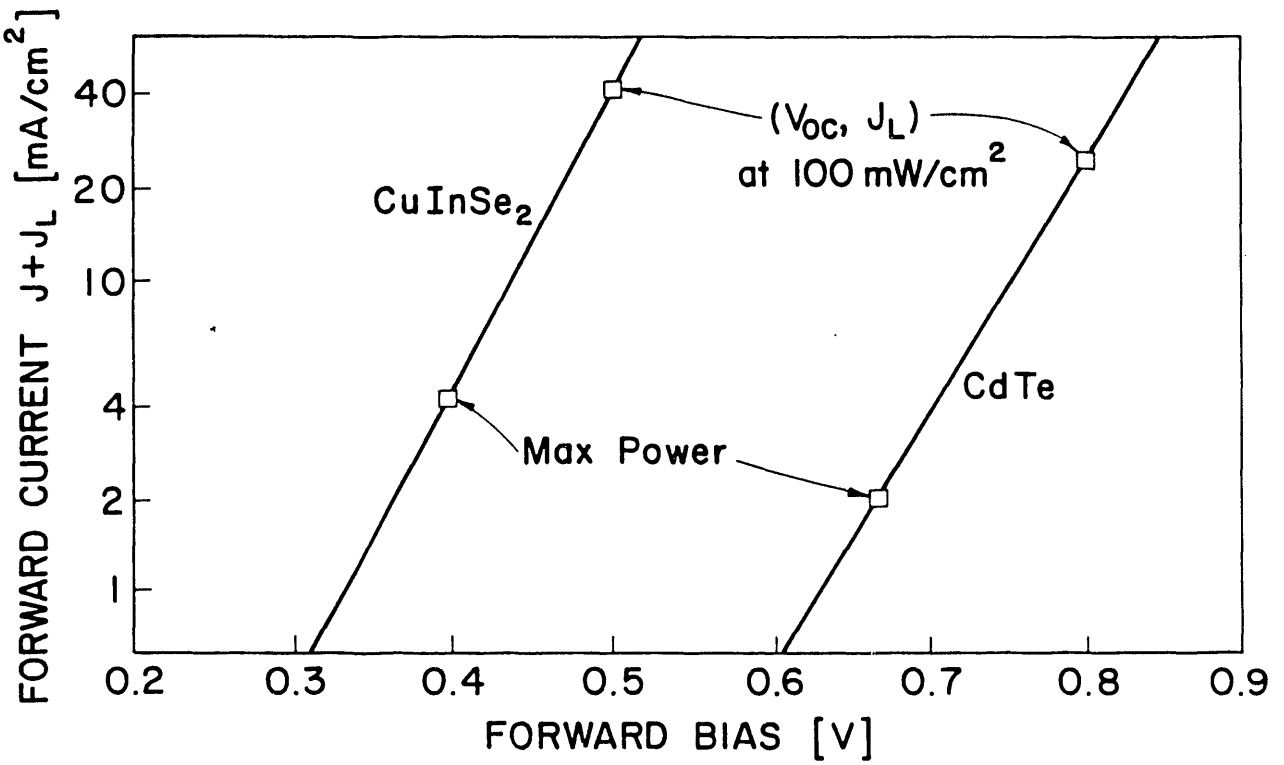

Fig. 2-1. Target-cell diode curves.

of curve is insensitive to photocurrent losses, and is hence useful for comparing the junction properties of diodes. When experimental data is superimposed on the target curve, one has a visual presentation of the problems associated with that junction. For example, Fig. 2-2 shows a set of experimental $CuInSe_2$ data, and the solid line exponential fit after series resistance R and shunt resistance r have been removed [2]. The effects of the individual parameters are shown. In many cases one or two parameters play a dominant role, and it is useful to identify them quickly and hopefully take corrective action.

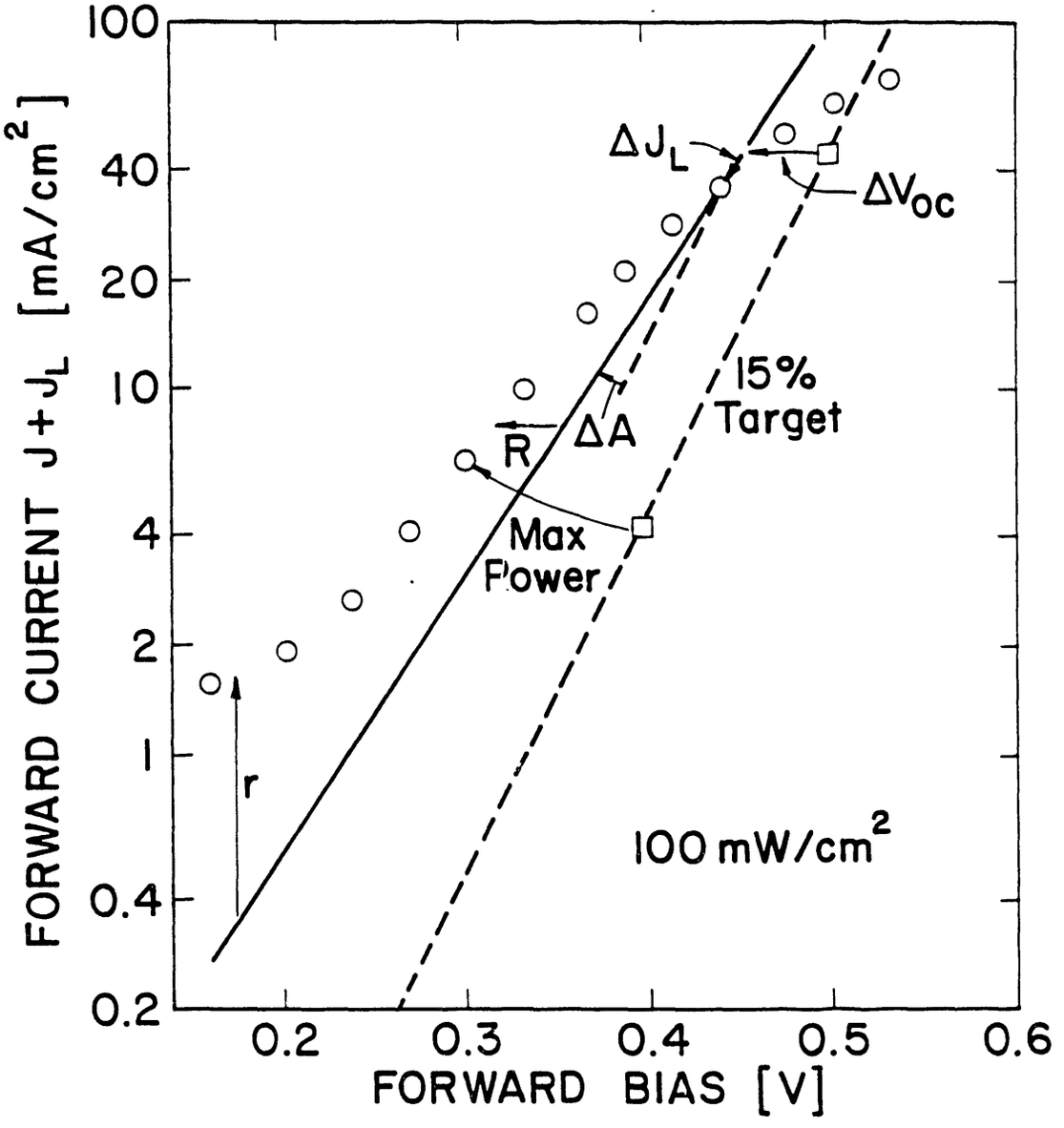

Fig. 2-2. Graphical presentation of forward current loss parameters.

3. CdTe CELLS

During the past year there has been significant progress on CdTe solar cells. The comparison here deals with five selected cells from the following laboratories: University of South Florida, Photon Energy, Microchemistry, Ltd. (Finland), Ametek Advanced Materials Lab, and Georgia Institute of Technology. Most of the data used came from SERI measurements, but some was taken in our laboratory or reported by the cell manufacturers.

Table 3-1 gives a numerical comparison of what we consider important cell parameters. The V_{OC}, J_L, ff, and efficiency numbers were generally reported by the manufacturer or SERI. Most of the other numbers were deduced by us. Figure 3-1 is a comparison of junction properties

Table 3-1. CdTe Cell Comparison

	USF	Photon Energy	Micro-Chemistry	Ametek	GIT
Cell Number	5-16-8-1	3	published	91A6-2	C224
Technique	CSS	Spray	ALE	Electrodep.	MOCVD
Efficiency (%)	13.4	12.7	11.5	11.0	10.3
V_{OC} (mV)	840	790	810	765	715
A-value	2.5	3.6	2.2	2.25	3.9
R (Ω-cm^2)	0.4	0.7	0.8	0.6	0.2
r (Ω-cm^2)	1500	600	1800	1400	700
V_{MP} (mV)	675	585	665	615	530
Fill Factor	0.725	0.615	0.73	0.715	0.60
J_L (mA/cm^2)	21.9	26.2	19.5*	20.9	24.2
Reflection Loss (mA/cm^2)	2	2	2	2	2
Window Loss (mA/cm^2)	2½	1	8	5	2½
Deep Loss (mA/cm^2)	1	1	1	1½	1
Unknown Loss (mA/cm^2)	3	½	---	1	½

*Adjusted to SERI measurement.

NOTE: J_L plus losses equals 30½ mA/cm^2.

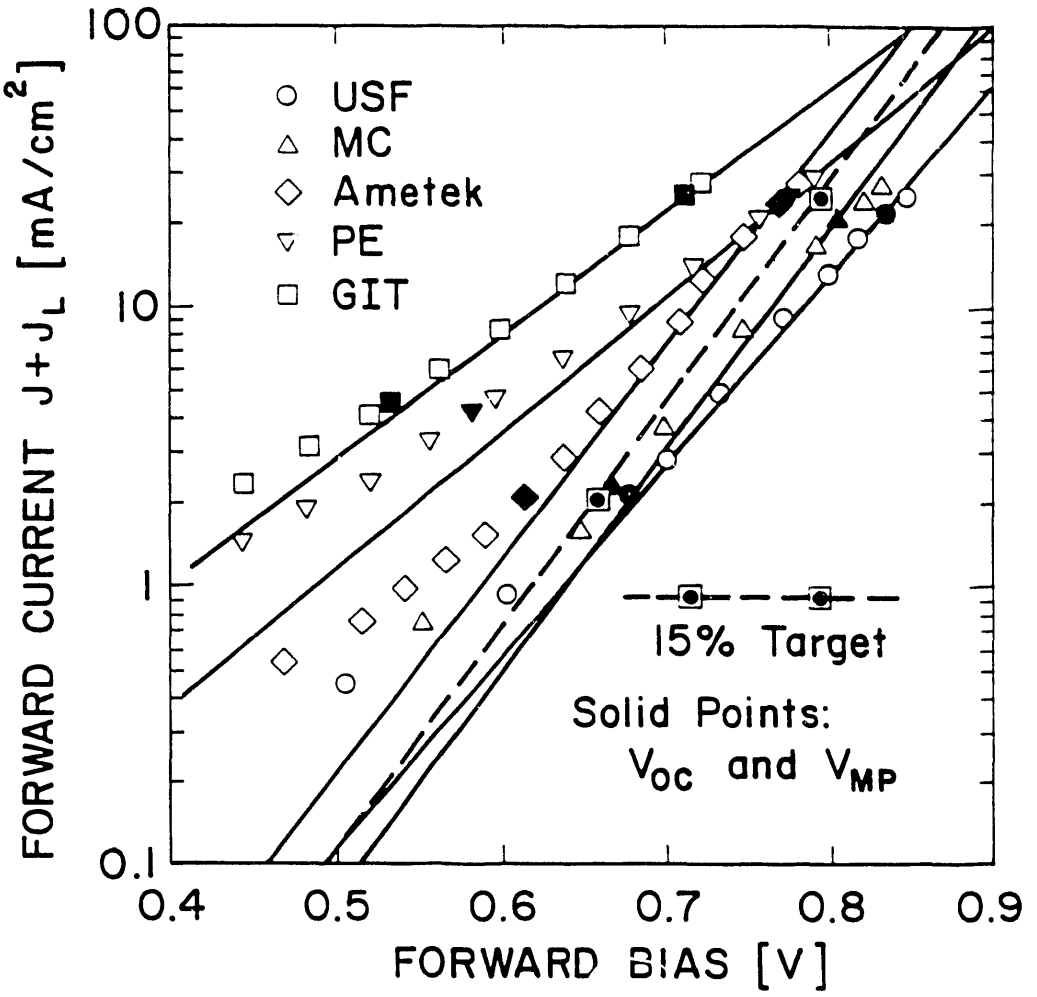

Fig. 3-1. Comparison of CdTe junctions.

based on plots of forward current under illumination vs. voltage. The dashed line is for the 15% target cell defined in Table 2-1. Figure 3-2 is a comparison of photocurrent losses based on quantum efficiency data. Figure 3-2 is normalized using the total photocurrent. The dashed line here is the expected reflection loss from a glass substrate. Most of the cells show only this loss at intermediate wavelengths.

University of South Florida. This cell with CdS solution grown and CdTe deposited by close space sublimination (CSS), has the highest SERI-confirmed CdTe efficiency to date. It has a very high V_{OC} combined with respectable value for diode quality factor A and series resistance R. This combination gives a very good fill factor and the highest maximum power voltage (675 mV) seen to date. (A companion cell with lower A-

factor reached 693 mV, but also had a smaller photocurrent). Graphically (Fig. 3-1) its forward-current curve is superior to our 15% target at both V_{OC} and V_{MP}. Its current, however, is only fair (Fig. 3-2). It has a reasonable window loss (2½ mA/cm^2), but it suffers an unknown loss (3 mA/cm^2) at mid-wavelengths. Optical measurement should determine whether this unknown loss is due to enhanced reflection or free electron window absorption.

Photon Energy. This cell has the highest confirmed photocurrent. The CdTe is deposited by a spray process. The window loss (Fig. 3-2) is quite small (1 mA/cm^2) due presumably to very thin CdS, and the mid-range and near bandgap losses are typical. This cell has respectable V_{OC} and R values, but its diode quality factor is high. Hence, (Fig. 3-1) its forward-current curve has a shallow slope reducing fill factor and V_{MP}.

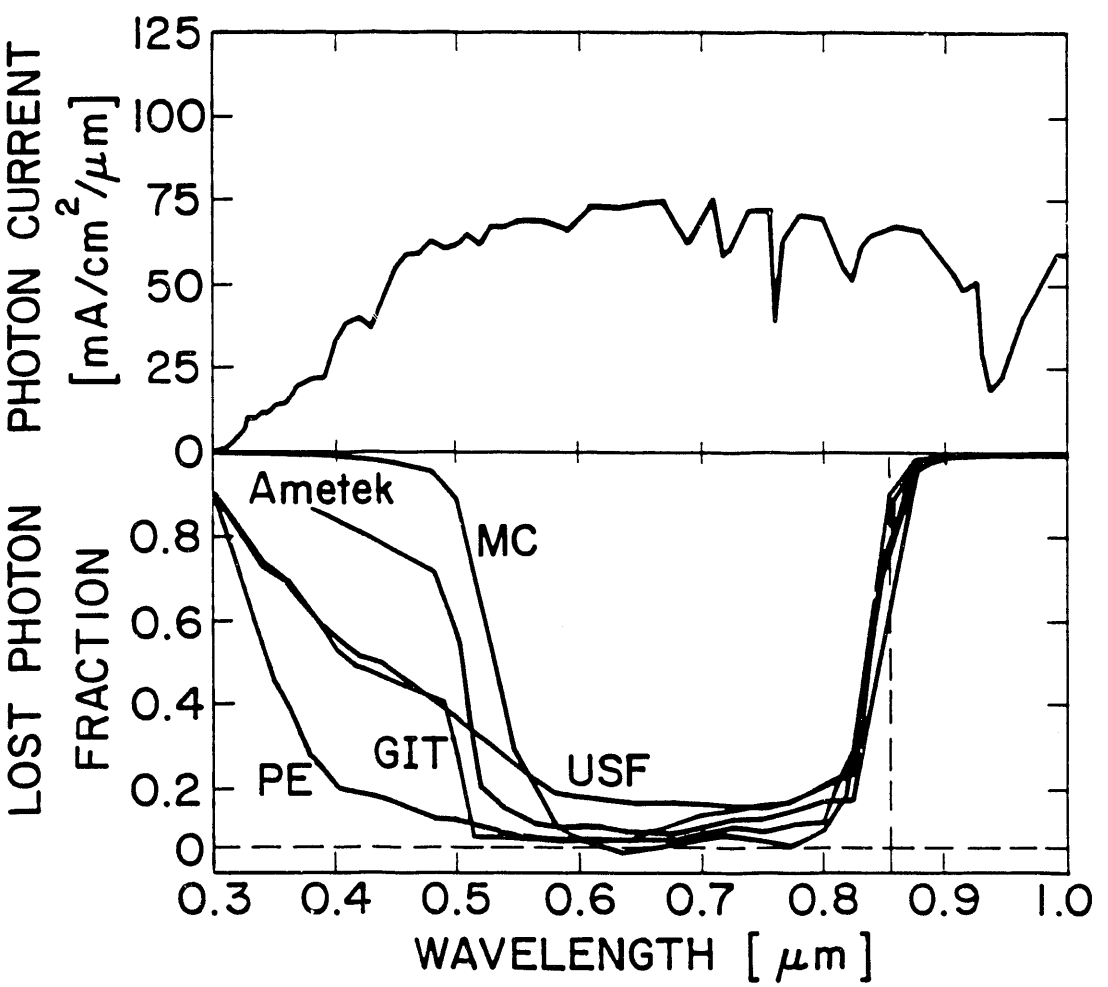

Fig. 3-2. Comparison of CdTe photocurrent losses.

Microchemistry. For our analysis we took the published data [3] normalized to photocurrent measured later at SERI. The reasoning is that the voltages measured in Finland should be reliable, but the photocurrent is sensitive to the correction for the spectrum used. Furthermore, the quantum efficiency measured at SERI (Fig. 3-2) normalizes very nicely to the reflection reference line, strongly suggesting that it has not experienced degradation. This cell was deposited by atomic layer epitaxy (ALE). The junction properties (Fig. 3-1) of this cell, V_{OC} and A, are quite good and its series resistance is fair. Hence its fill factor is slightly above and its V_{MP} only slightly below the USF cell. Window absorption (8 mA/cm^2), however, is higher than one would expect from thick CdS and possibly results from a reduced window-bandgap due to a wider region of CdTe-CdS grading than that produced by other manufacturers.

Ametek. The best electrodeposited Ametek cells had junction properties similar to the USF and MC, Ltd. cells, but with smaller values of V_{OC} (Fig. 3-1). Their photocurrent losses (Fig. 3-2) are typical of relatively thick CdS (5 mA/cm^2) with a little more loss corresponding to deeply penetrating photons (1½ mA/cm^2) than we see with the other cells.

Georgia Tech. This cell used metal-organic chemical vapor deposited (MOCVD) CdTe. Its photocurrent is reasonably good (Fig. 3-2) with window loss (2½ mA/cm^2) suggestive of intermediate thickness CdS and only modest losses otherwise. It is also fabricated with a low series resistance. Its junction properties, however, are the weakest of the five cells. V_{OC} is low and the diode quality factor high, leading (Fig. 3-1) to a maximum power voltage less than 80% of the USF cell.

Composite. If one could combine the photocurrent achieved by Photon Energy with the other parameters from the best USF cell, the cell efficiency would be 15.9%. Alternatively, if one combines the Photon Energy photocurrent with the highest V_{MP} USF cell, the efficiency reaches 16.3%. There is no obvious reason why such a combination is not feasible in the near future.

4. $CuInSe_2$ CELLS

The highest reported efficiency for $CuInSe_2$ cells remains the 14.1% reported by ARCO Solar in 1988 [4]. This cell achieved a very high photocurrent density (41 mA/cm^2) through very low reflection and window absorption. During the past year, the primary reported progress has been with the junction properties attained by International Solar Electric Technology (ISET).

Figure 4-1 shows the light and dark forward currents from ISET cell 489, which has the lowest forward current to date in the 100 mW/cm^2 operating

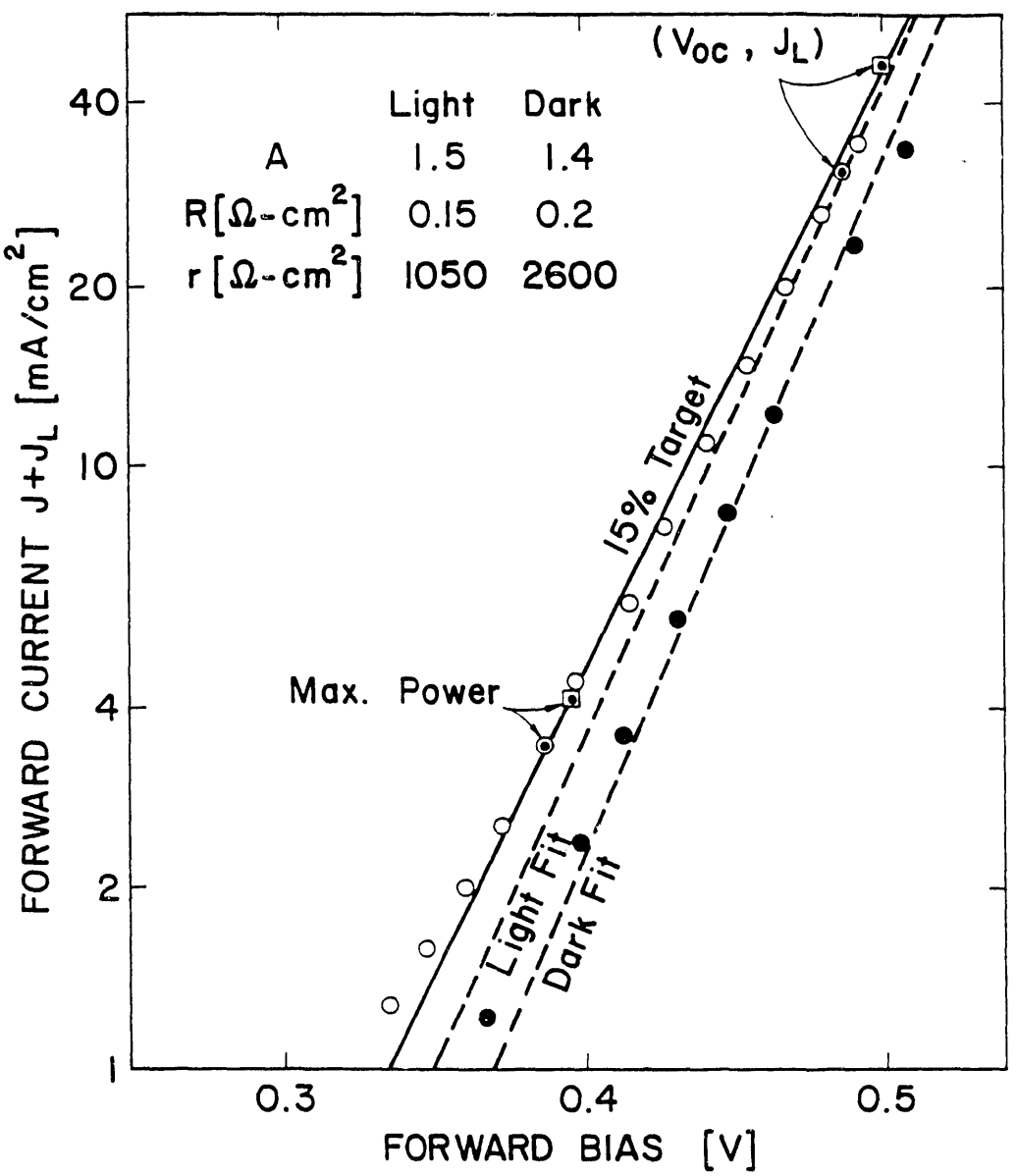

Fig. 4-1. Light and dark forward currents from best ISET junction.

range, our working definition of junction quality. The detailed measurements were made in our lab, but the light current-voltage curve confirmed at SERI. In this case the solid line is our 15% target with squares denoting maximum power and V_{OC}. The dark points fall clearly to the right of the 15% target curve and the light ones marginally to the right. Both light and dark curves have small series resistance R, fair shunt resistance r, and quite low diode quality factor A. Hence they exhibit a large (0.715) fill factor for their bandgap. The difference between the light and dark fits is about 15 mV, implying that superposition is quite good. The two significant problems with the cell, high reflection and high free electron absorption in the ZnO part of the window, held the photocurrent below 33 mA/cm^2 and the efficiency to 11.3%.

The A-factor for the cell shown in Fig. 4-1 is not constant with the temperature. Figure 4-2 shows its variation, with the open light points always slightly larger than the dark ones.

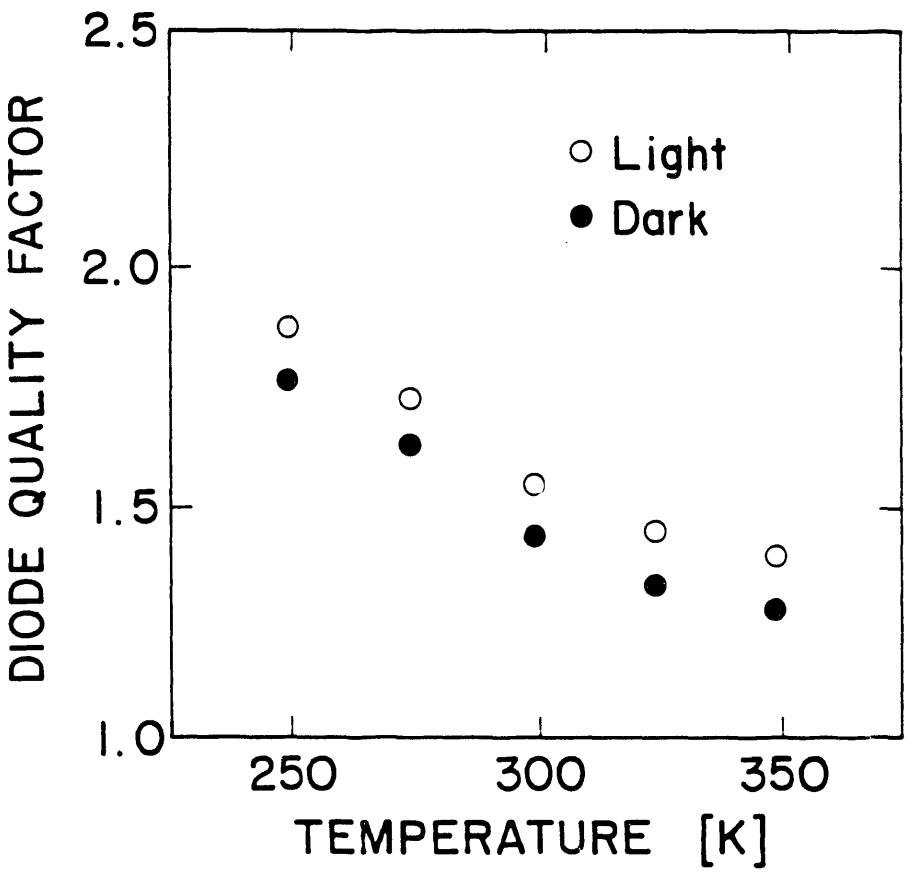

Fig. 4-2. Variation in light and dark A-factors with temperature. ISET cell 489.

Another feature of the improved junction cell is that the $CuInSe_2$ hole density, as deduced from reverse bias C^{-2} vs. V curves, is over a factor of 2 higher than that seen in any other $CuInSe_2$ cell. The large value, 7×10^{16} cm^{-3}, is interpreted as the result of significantly reduced compensation. Figure 4-3 shows the correlation of botn hole density and A-factor with open circuit voltage for several ISET cells fabricated

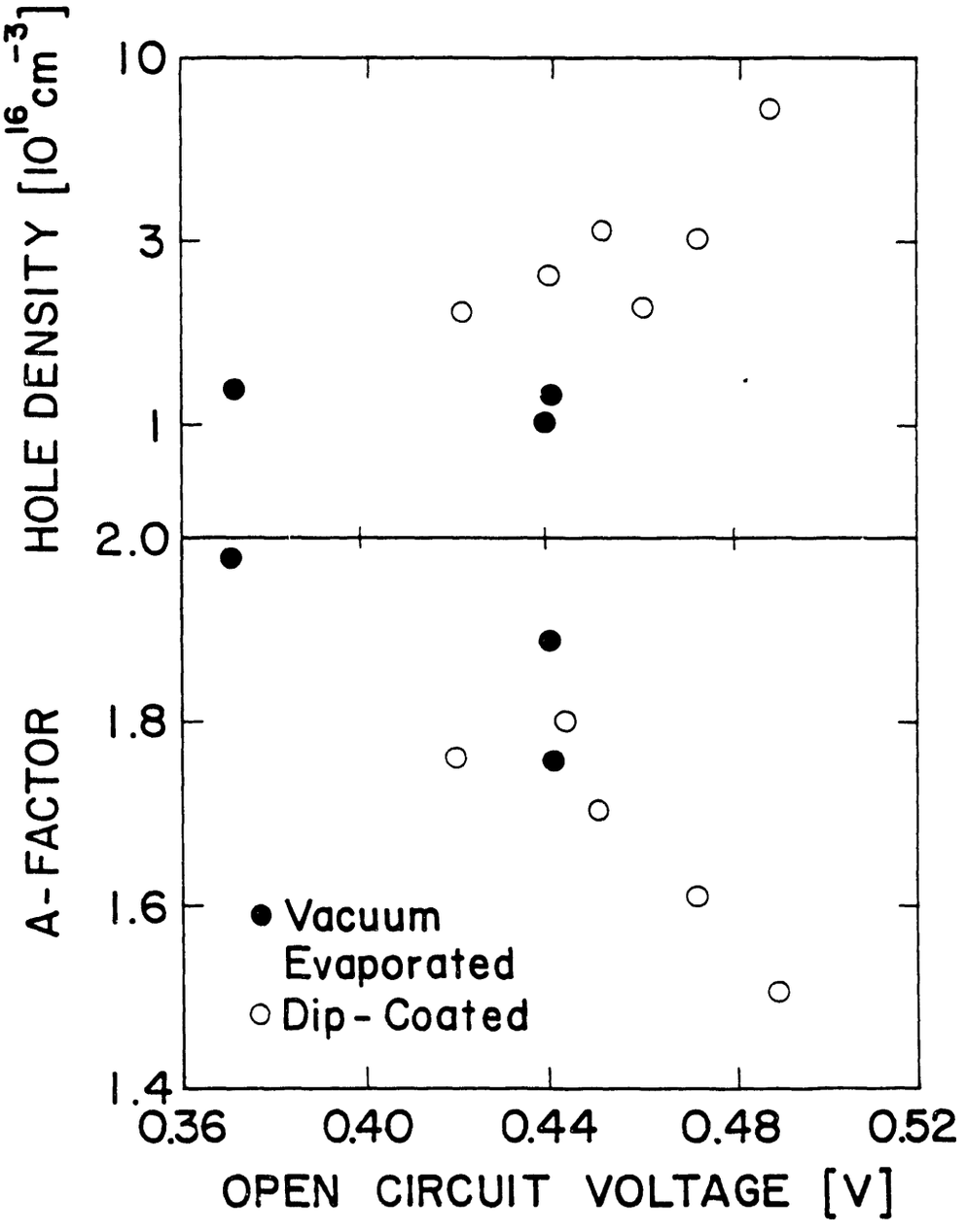

Fig. 4-3. Correlation of hole density and A-factor with V_{OC} for several ISET cells.

during the last year. Cell 489 is at the far right. The overall trends imply that the better junctions have fewer recombination centers in the depletion region. Hence these junctions have both lower compensation and a recombination mechanism that looks progressively less like Shockley-Read-Hall. The A-factor trend shown with these cells, incidentally, is opposite to that seen in IEC cells by Shafarman et al. [5].

Also shown in Fig. 4-3 is the contrast between $CuInSe_2$ which is overlaid with vacuum-evaporated CdS compared to that with dip-coated CdS. It suggests that the vacuum evaporation process tends toward more compensation in the junction part of the $CuInSe_2$. A second, and more obvious, contrast between the two deposition techniques is shown in Fig. 4-4. The top curves are the photon losses from four cells, plotted as in Fig. 3-2. The dip-coated cells clearly generate significant photocurrent at smaller wavelengths. The bottom curves, which include these and five other cells, show that the dip coating leads to a photocurrent loss nearly 2 mA/cm^2 less than the vacuum evaporation for equal thickness CdS. There are several possible explanations, but we think it most likely that photogenerated holes in the relatively good quality dip-coated CdS are contributing to the photocurrent.

5. $CuInSe_2$ ANNEALING STUDY

The need for post-deposition annealing of $CuInSe_2$ cells with vacuum evaporated $CuInSe_2$ has been recognized for some time. Building on an earlier study [6], we have explored how the individual parameters change with annealing temperature [7]. The cells used were fabricated by vacuum evaporation at the Institute for Energy Conversion (IEC), University of Delaware.

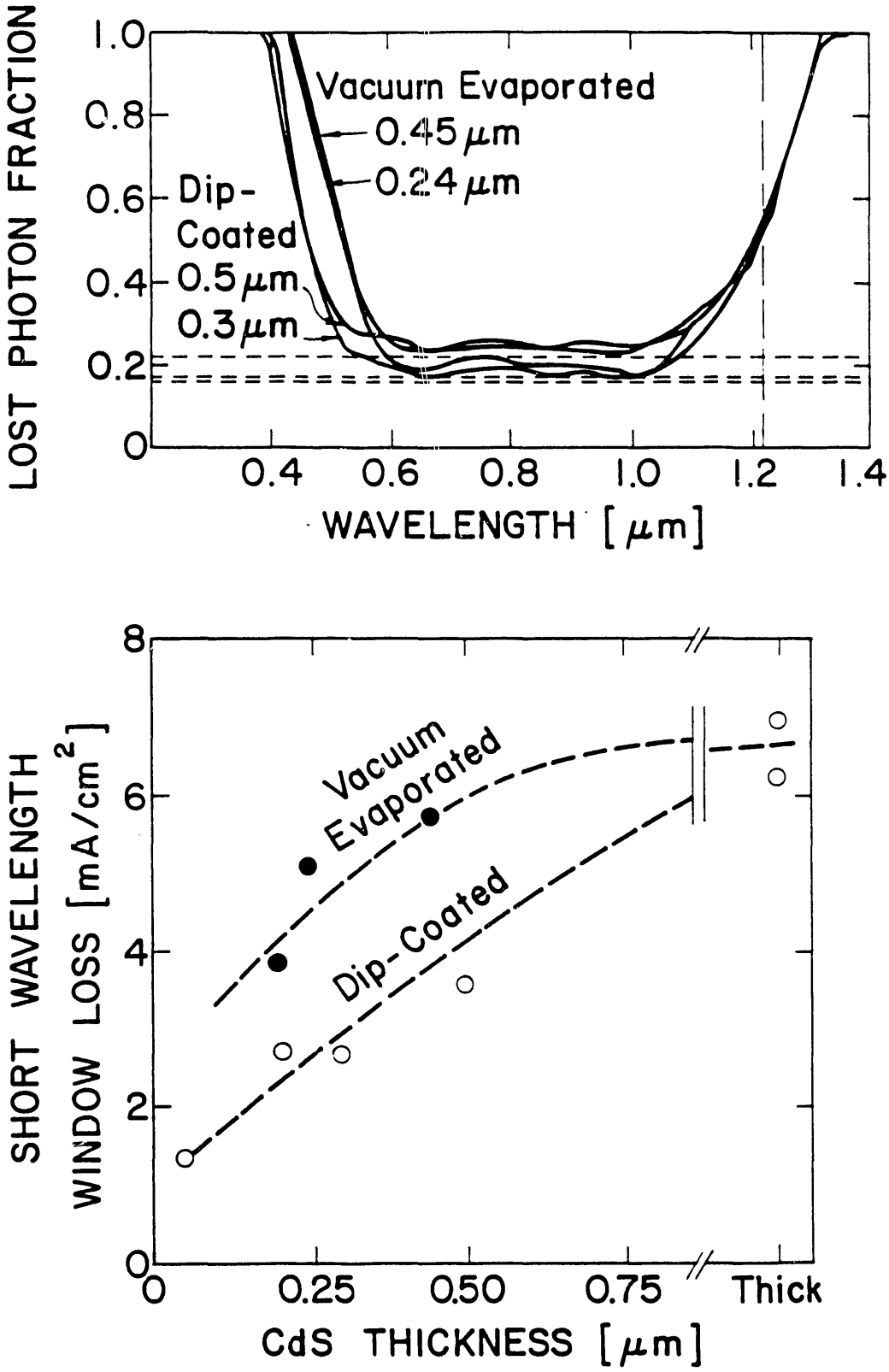

Fig. 4-4. Contrast between absorption losses in vacuum evaporated and dip-coated CdS cells.

Figure 5-1 shows the current voltage curves following anneals of several temperatures. The cells improved after they were heated at temperatures up to 275°C, after which the cells began to degrade rapidly, becoming nearly ohmic and insensitive to light at 350°C. This degradation has been noted previously. It is caused by a combination of higher series resistance, lower shunt resistance, larger forward recombination current, and a lower photogenerated current.

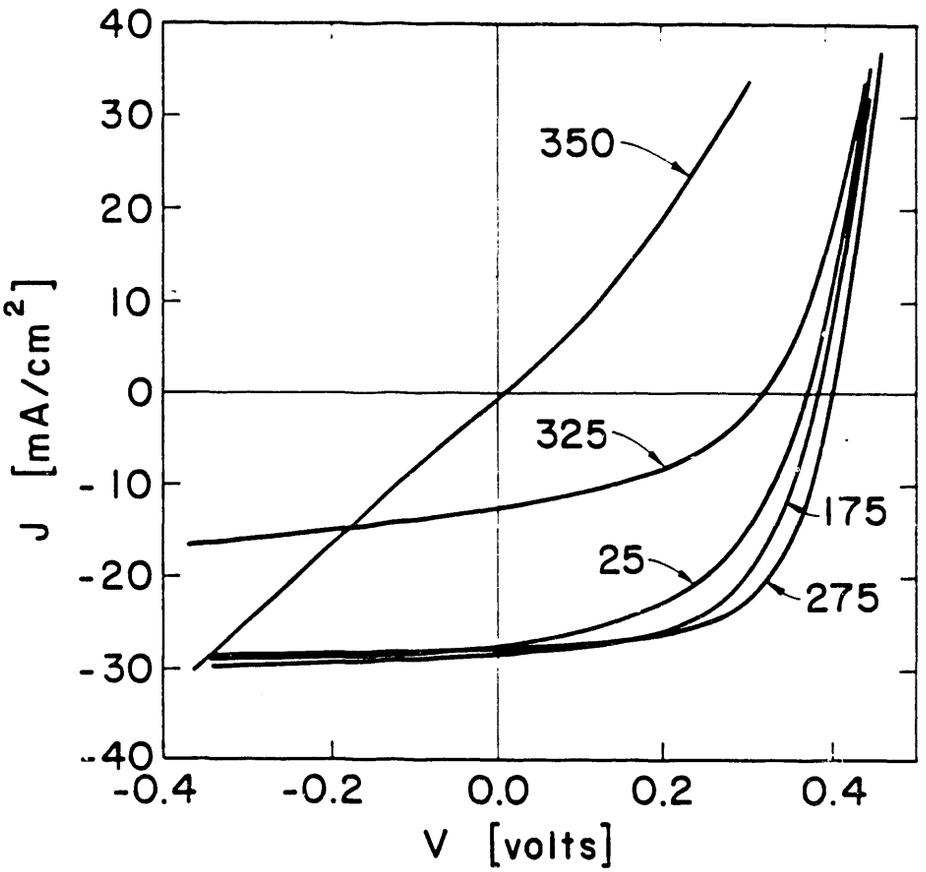

Fig. 5-1. Current-voltage curves for an IEC cell following anneals at the temperatures indicated.

In Fig. 5-2 room temperature values of J_{SC} and V_{OC} vs. annealing temperature (T_A) are plotted. Changes in J_{SC} were not a strong function of spectral content. The curves roughly track each other. They both rise slowly at low T_A and decline rapidly for high T_A. However, J_{SC} begins its decline at 250°C, whereas V_{OC} starts to drop at 300°C. Note that the maximum value of J_{SC} occurs at 225°C which is generally cited as the optimum anneal temperature [8]. The implication of different

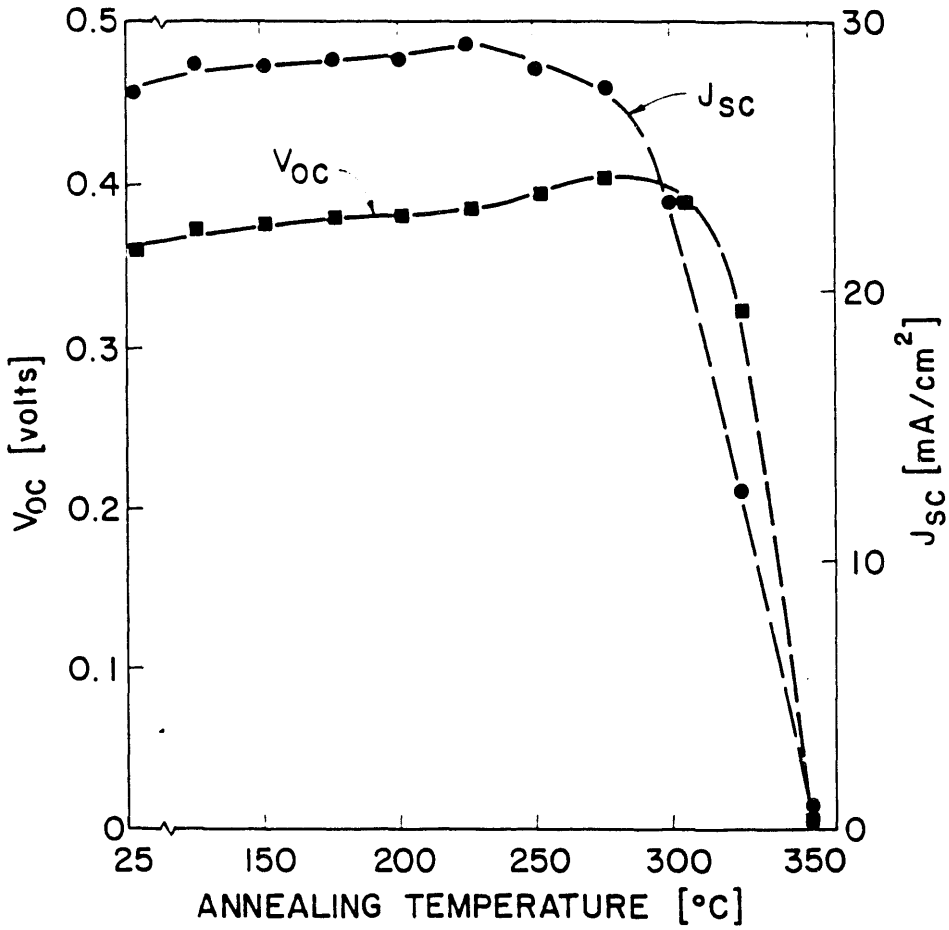

Fig. 5-2. Variation of J_{SC} and V_{OC} with annealing temperature.

onset temperatures for the decrease in V_{OC} and J_{SC} is that more than one physical mechanism is present.

To help separate the degradation mechanisms, the annealing effects on the diode quality factor A, the shunt resistance r_S, and series resistance R_S are examined separately, as shown in Fig. 5-3. There is a positive correlation between the value of A and the amount of forward recombination current. The forward current opposes the photogenerated current, and any increase results in lower operating voltages. In Fig. 5-3a, the diode quality factor decreases between 175°C to 275°C, exactly the same region that V_{OC} increases in Fig. 5-2. The increase in V_{OC} is due to lower recombination, and most likely corresponds, on the microscopic level, to oxygen passivation of grain boundary defects.

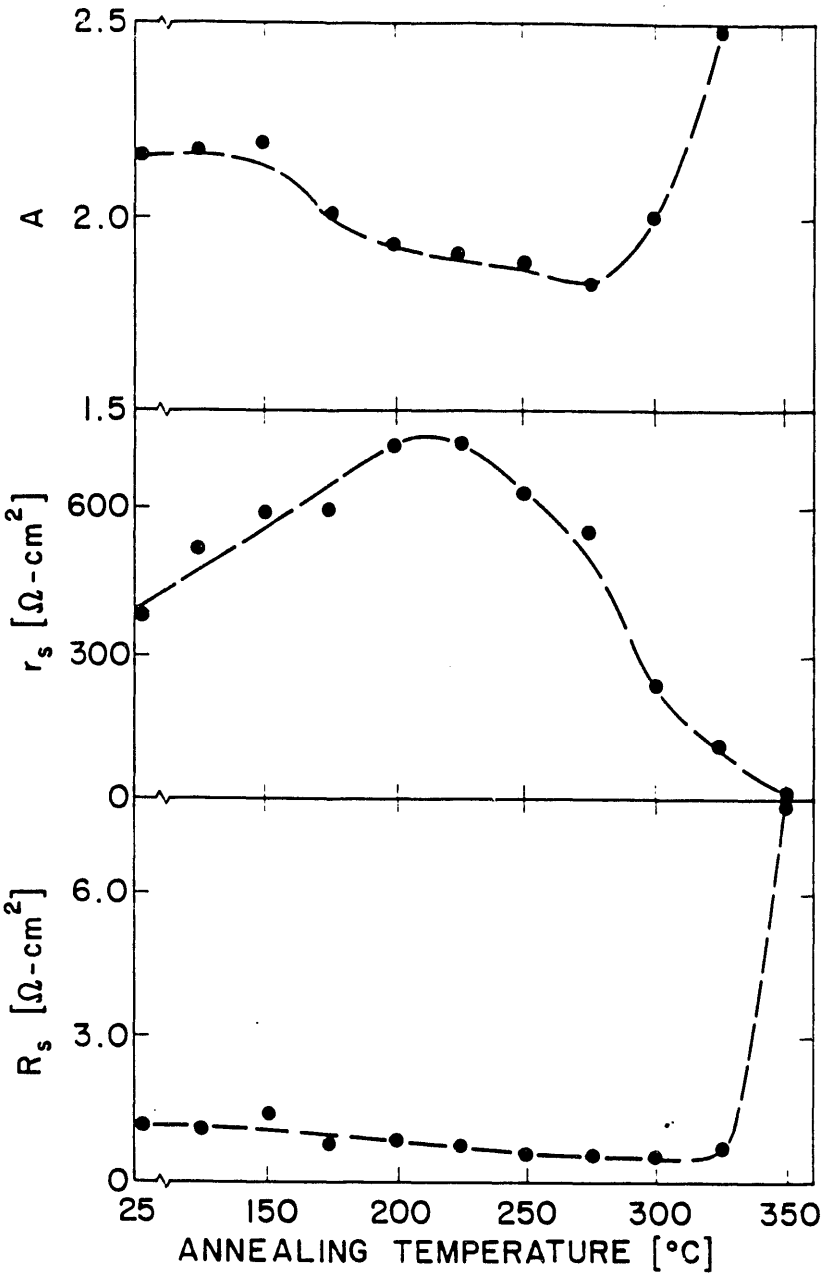

Fig. 5-3. Variation of diode quality factor, shunt resistance and series resistance with anneal temperature.

Degradation of the solar cell is first seen in the shunt resistance, as shown in Fig. 5-3b. The shunt resistance increases with annealing temperature up to 200°C. The increase is due to a reduction in leakage current probably related to the oxidation of grain boundary defects. As the temperature is increased past 225°C, the shunt resistance trend reverses and it begins to decline. As the temperature is increased to 300°C, leakage becomes extensive and the shunt resistance drops quickly.

The series resistance, plotted in Fig. 5-3c, closely follows the trend of A. The decrease in the series resistance is due to an increase in mobility which follows from the decrease in defects. As the temperature is increased past 300°C, the mobility falls rapidly resulting in a large series resistance increase.

Figure 5-4a shows the intrinsic layer thickness as a function of annealing temperature. Note that a measurable intrinsic layer first develops at 275°C and grows rapidly at higher temperatures. The intrinsic thickness at 350°C is about 1.5 μm which is half the thickness of the $CuInSe_2$ layer.

The hole density increases steadily with annealing temperature, as shown in Fig. 5-4b. This increase of p corroborates the thesis that compensating donor states are eliminated through oxidation at the lower annealing temperatures. As the temperature is increased beyond 275°C and S and Se diffuse across the junction, one might expect the hole density to decrease. This decrease, however, is not apparent in the capacitance data, since as the intrinsic layer develops, the depletion region is moved deeper into the $CuInSe_2$. Thus, a different physical region is probed. The dashed line in Fig. 5-4b represents the anticipated result if the same physical region were measured.

The number of extraneous states, N_{ES}, in the depletion region is proportional to the difference in capacitance measured at high and low frequencies [9]. In Fig. 5-4c, N_{ES} vs. annealing temperature is plotted. As expected, N_{ES} decreases with annealing temperature until reaching a minimum at 250°C. This corresponds to the reduction of compensating donor defects discussed above. Note that care must be used in interpreting N_{ES} at temperatures above 275°C, because of the development of the intrinsic layer. The dashed line in Fig. 5-4c is the expected result in the absence of an intrinsic layer.

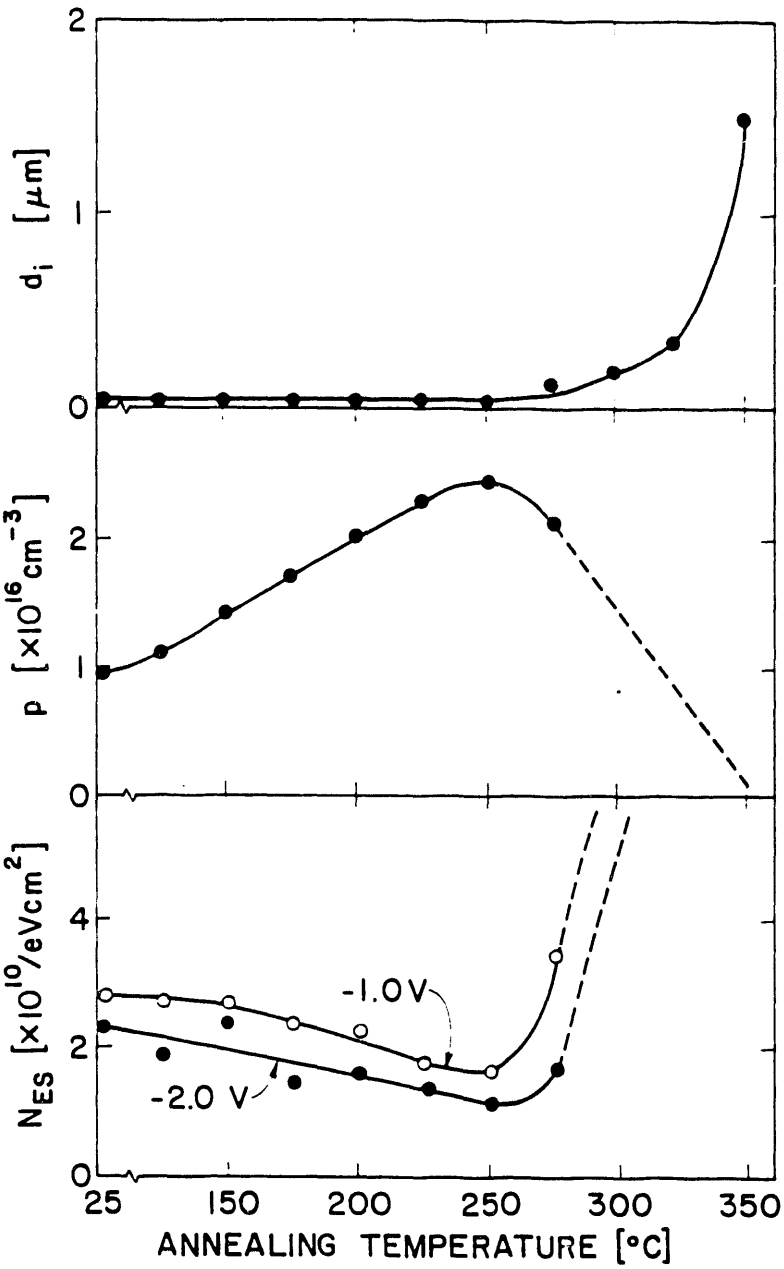

Fig. 5-4. Intrinsic layer thickness d_i, hole density p, and extraneous state density N_{ES}, all deduced from dark capacitance data.

Annealing effects on other evaporated and selenized $CuInSe_2$ cells have been studied less extensively. The general degradation patterns shown above are always present, but the onset of degradation can occur at significantly lower temperature. Additional study, particularly with selenized cells, is therefore needed to see whether fabrication

procedures, type of window, or other factors have an inherent effect on the degradation process.

6. MEASUREMENT FACILITY IMPROVEMENTS

Quantum Efficiency. A new filter wheel arrangement with a wider wavelength range (400-1300 nm) has been constructed. As shown in Fig. 6-1, the quantum efficiency measurements are made with the cell

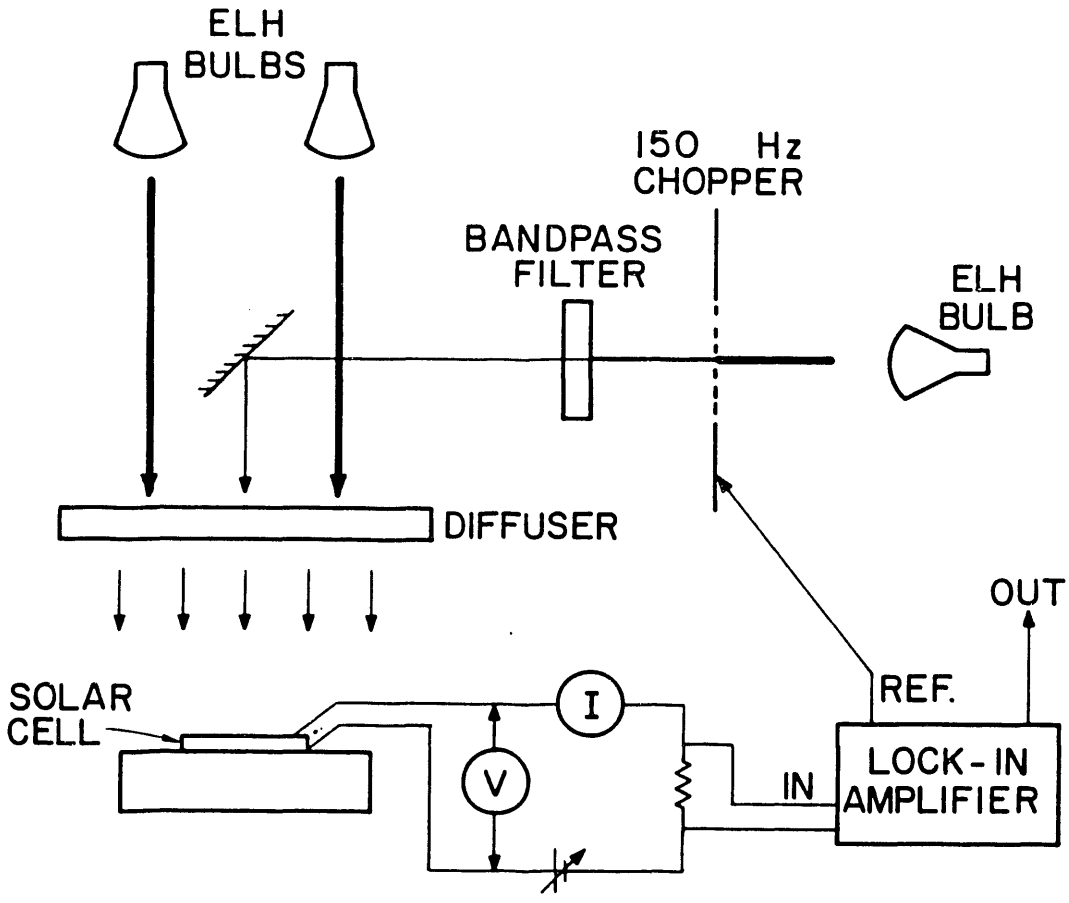

Fig. 6-1. Quantum efficiency measurement system.

mounted in its standard current-voltage configuration. Each filter is individually calibrated from quantum efficiency measurements at SERI on multiple reference cells. The quantum efficiency normalization for each cell tested requires the integrated product of quantum efficiency and photon spectrum to equal the measured photocurrent.

Circuit Resistance. We have replaced our contact micropositioners with higher quality models and now routinely operate in a four-wire

configuration with cells larger than 0.2 cm^2. Consequently, our I-V curves should not have any significant distortion due to extraneous circuit resistance.

Temperature Effects. We noted fairly significant temperature effects (~5°C) particularly with thin film cells on glass substrates, when 100 mW/cm^2 illumination was used for longer than a minute. A partial solution involved a fan in the light box, which slowed the temperature increase. Now we use cold flowing nitrogen gas to stabilize the temperature at 25°, as well as lower temperatures when desired. Stabilization to less than 1°C is seen in the voltage of a thermocouple, the open circuit voltage of polycrystalline cells, and the open circuit voltage of our silicon reference cells.

Time Dependence. We have recently acquired a two-channel digitizing oscilloscope and have set up the computer link to measure transient effects following an abrupt change in illumination on voltage. Figure 6-2 shows the configuration to chop a laser beam quickly by putting a rapid

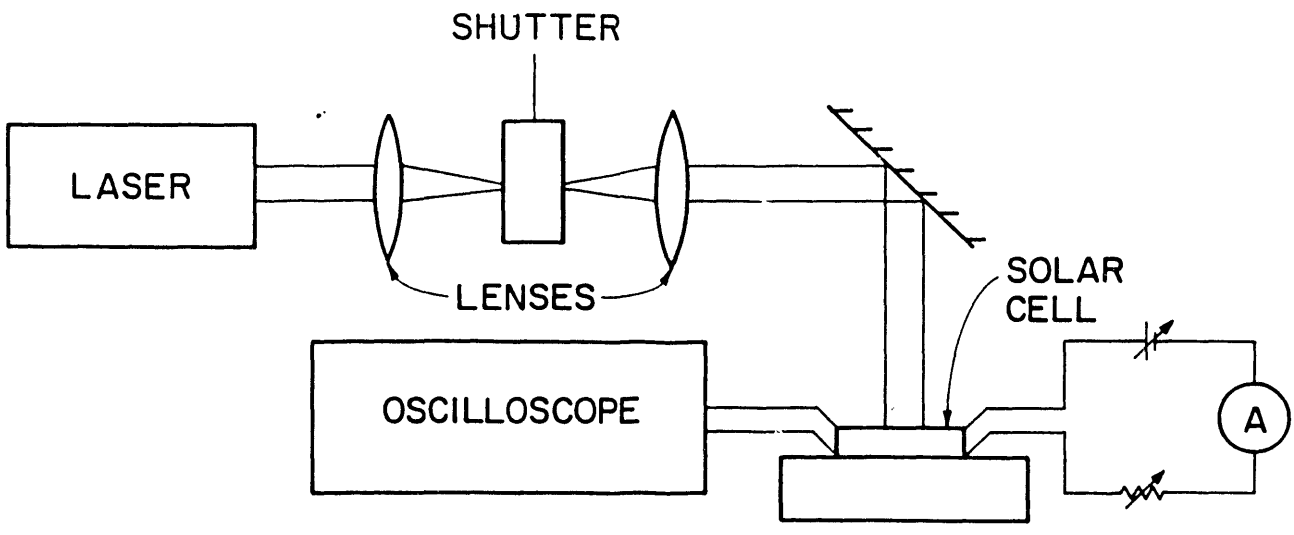

Fig. 6-2. Abrupt on-off control of solar cell illumination.

shutter in the focal plane of the two lenses. The system also works with white light, but since the focal image is larger, the on-off time is proportionally longer.

7. RECOMMENDATIONS

We continue to recommend systematic and quantitative analysis of solar cell loss mechanisms. It is important for all cell manufacturers to know in some detail what is working well and where the problems lie. We especially recommend routine extraction of series and shunt resistance under illumination, since they can vary significantly among similar cells and can unnecessarily complicate the analysis of more intrinsic parameters.

For CdTe, the obvious recommendation is to explore whether the junctions produced by the University of South Florida and Microchemistry, Ltd., can be combined with the low window absorption by Photon Energy while keeping the series resistance low. Similarly, with $CuInSe_2$, a serious effort should be made to combine the best features in a single cell.

As the quality of polycrystalline cells improves, greater attention to contacting is suggested. Often we find that a cell measured both at SERI and another lab (including until recently our own) will show a greater series resistance in the non-SERI measurement. Probe resistance is typically 1Ω, which is significant for cells with area greater than ~0.2 cm^2. Furthermore, some investigators continue to identify dV/dJ at V_{oc} as the series resistance, an overestimate of ~2Ω-cm^2[2]. Another measurement area that needs more attention is temperature, which can drift considerably during illuminated measurement. We recommend monitoring V_{oc} in a cell, similar to the one under study, where V_{oc} vs. T has been previously calibrated.

8. COMMUNICATIONS

8.1 Publications

1. "Individual Losses in Thin-Film CdTe Solar Cells," Proc. 21st IEEE Photovoltaics Specialists Conf., p. 556 (1990).

2. "Annealing Effects on individual Loss Mechanisms in $CuInSe_2$ Solar Cells," Solar Cells 29, 101 (1991).

8.2 Talks

1. PVSC21, Orlando, FL — May 27, 1990
2. PVAR&D10, Denver, CO — October 23, 1990
3. Solarex, Newtown, PA — February 6, 1991

9. REFERENCES

[1] R. Hulstrom, R. Bird, and C. Riordan, "Spectral Solar Irradiance Data Sets for Selected Terrestrial Conditions" (Table 2b), Solar Cells 15, 365 (1985).

[2] J. R. Sites and P. H. Mauk, "Diode Quality Factor Determination for Thin-Film Solar Cells," Solar Cells 27, 441 (1989).

[3] J. Skarp, Y. Kosiner, S. Lindfors, A. Rautiainen, and T. Suntola, "Development and Evaluation of Cds/CdTe Thin Film PV Cells," Proc. 10th European Photovoltaic Conf., Lisbon, 1991.

[4] K. W. Mitchell, C. Eberspacher, J. Ermer, and D. Pier, "Single and Tandem Junction $CuInSe_2$ Cell and Module Technology," Proc. 20th IEEE Photovoltaic Specialists Conf., Las Vegas, 1988, p. 1604.

[5] W. N. Shafarman, R. W. Birkmire, D. A. Fardig, B. E. McCandless, A. Mondal, J. E. Phillips, and R. D. Varrin, Jr., "Advances in $CuInSe_2$ and CdTe Thin Film Solar Cells," Solar Cells 30, 69 (1991).

[6] R. E. Hollingsworth and J. R. Sites, "Annealing Temperature Effects on $CuInSe_2$/CdS Solar Cells," Solar Cells 16, 457 (1986).

[7] R. A. Sasala and J. R. Sites, "Annealing Effects on Individual Loss Mechanisms in $CuInSe_2$ Solar Cells," Solar Cells 30, 101 (1991).

[8] R. J. Matson, C. R. Herrington, R. Noufi, and R. C. Powell, "EBIC Studies of Junction Formation and the Role of Oxygen in Thin-Film CdS/$CuInSe_2$ Solar Cells," Proc. 18th IEEE Photovoltaics Specialists Conf., Las Vegas, 1985, p. 1648.

[9] J. R. Sites, H. Tavakolian, and P. H. Mauk, "Interpretation of Thin-Film Polycrystalline Solar Cell Capacitance," IEEE Trans. Electron Devices ED-37, 442 (1990).

Document Control Page	1. SERI Report No. SERI/TP-214-4468	2. NTIS Accession No. DE92001168	3. Recipient's Accession No.

4. Title and Subtitle
Role of Polycrystallinity in CdTe and $CuInSe_2$ Photovoltaic Cells; Annual Subcontract Report, April 1, 1990 - March 31, 1991

5. Publication Date
November 1991

6.

7. Author(s)
J. R. Sites

8. Performing Organization Rept. No.

9. Performing Organization Name and Address
Department of Physics
Colorado State University
Fort Collins, Colorado 80523

10. Project/Task/Work Unit No.
PV131101

11. Contract (C) or Grant (G) No.
(C) XC-0-10046-1
(G)

12. Sponsoring Organization Name and Address
National Renewable Energy Laboratory
1617 Cole Blvd.
Golden, Colorado 80401-3393

13. Type of Report & Period Covered
Technical Report

14.

15. Supplementary Notes
NREL Technical Monitor: H.S. Ullal, (303) 231-1486

16. Abstract (Limit: 200 words)
The polycrystalline nature of thin-film CdTe and $CuInSe_2$ solar cells continues to be a major factor in several individual losses that limit overall cell efficiency. This report describes progress in the quantitative separation of these losses, including both measurement and analysis procedures. It also applies these techniques to several individual cells to help document the overall progress with CdTe and $CuInSe_2$ cells. Notably, CdTe cells from Photon Energy have reduced window photocurrent losses to 1 mA/cm^2; those from the University of South Florida have achieved a maximum power voltage of 693 mV; and $CuInSe_2$ cells from International Solar Electric Technology have shown a hole density as high as 7×10^{16} cm^{-3}, implying a significant reduction in compensation.

17. Document Analysis
a. Descriptors
Photovoltaic cells ; polycrystalline thin films ; cadmium telluride ; copper indium diselenide ; cell efficiency ; solar cells

b. Identifiers/Open-Ended Terms

c. UC Categories
273

18. Availability Statement
National Technical Information Service
U.S. Department of Commerce
5285 Port Royal Road
Springfield, VA 22161

19. No. of Pages
29

20. Price
A03

Form No. 0069E (6-30-87)

END

DATE
FILMED
2/07/92

I